A Non-perturbing Probe of Coiled Coil Formation Based on Electron Transfer Mediated Fluorescence Quenching

Matthew D. Watson,[a] *Ivan Peran,*[a] *Daniel P. Raleigh**[a,b]

[a] Department of Chemistry, Stony Brook University, Stony Brook, New York 11794-3400, USA

[b] Graduate Program in Biochemistry & Structural Biology, Stony Brook University, Stony Brook, New York 11794-3400, USA

KEYWORDS coiled-coil, p-cyanophenylalanine, selenomethionine, fluorescence quenching

ABSTRACT Coiled coils are abundant in nature, occurring in ~3% of proteins across sequenced genomes and are found in proteins ranging from transcription factors to structural proteins. The motif continues to be an important model system for understanding protein-protein interactions and is finding increased use in bio-inspired materials and in synthetic biology. Knowledge of the thermodynamics of self-assembly, particularly the dissociation constant K_D, is essential for the application of designed coiled coils and for understanding the *in vivo* specificity of natural coiled coils. Standard methods for measuring K_D typically rely on concentration dependent circular dichroism (CD). Fluorescence methods are an attractive alternative, however Trp is rarely found in an interior position of a coiled coil and appending unnatural fluorophores can perturb the system. We demonstrate a simple, non-perturbing method to monitor coiled coil formation using *p*-cyanophenylalanine (F_{CN}) and selenomethionine (M_{Se}), the Se analogue of Met. F_{CN} fluorescence can be selectively excited and is effectively quenched by electron transfer with M_{Se}. Both F_{CN} and M_{Se} represent minimally perturbing substitutions in coiled coils. M_{Se} quenching of F_{CN} fluorescence is shown to offer a non-perturbing method for following coiled coil formation and for accurately determining dissociation constants. The method is validated using a designed heterodimeric coiled coil. The K_D deduced by fluorescence monitored titration is in excellent agreement with the value deduced from concentration dependent CD measurements to within the uncertainty of the measurement. However, the fluorescence approach requires less protein, is less time consuming, can be applied to lower concentrations and could be applied to high throughput screens.

Protein-protein interactions are fundamental to the understanding of both normal protein function and many deleterious processes associated with disease. The coiled coil is one of the most common and important oligomerization motifs found in biology. This well-defined and extensively characterized fold comprises two or more α-helices twisted into a left-handed superhelix stabilized by a hydrophobic core.[1] Coiled coils are abundant in nature, occurring on average in ~3% of proteins across sequenced genomes and are found in proteins ranging from transcription factors to structural proteins.[2] They continue to be important model systems for understanding protein-protein interaction motifs, have been the focus of a large body of work on *de novo* protein design and are finding increased use in bio-inspired materials and synthetic biology.[3-9]

Coiled coil systems are also useful as test systems for the development of techniques for the study of protein-protein interactions. The system lends itself particularly well to the development of methods for non-invasive determination of dissociation constants (K_D), with the extent of association controllable by temperature, concentration of the individual peptides or the presence of denaturing agents.[8] Determination of K_D is also an important concern in the *de novo* design of coiled coil systems, which are an attractive target for functional protein engineering.[4, 5]

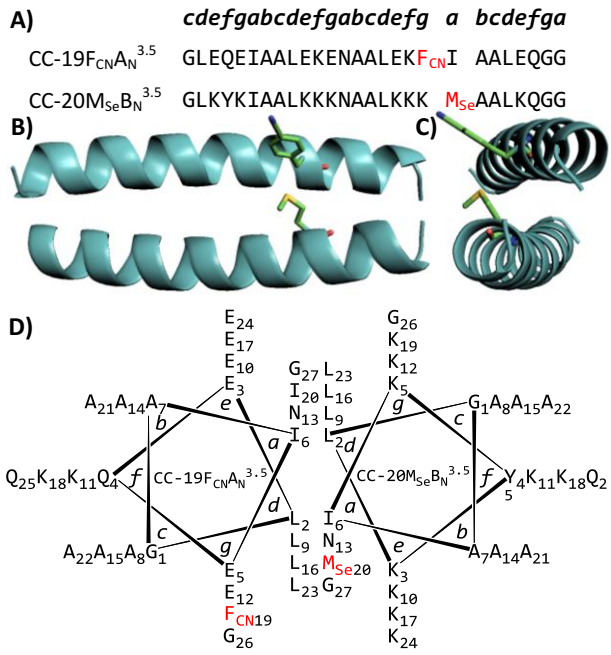

Figure 1. (A) Sequences and heptad register of the coiled coil peptides. These constructs were designated CC-19$F_{CN}A_N^{3.5}$ and CC-20$M_{Se}B_N^{3.5}$ (coiled coil, acidic or basic, Asn, 3.5 heptad repeats) after the system used by Thomas *et al.*[10] F_{CN} denotes *p*-cyanophenylalanine and M_{Se} denotes selenomethionine. **(B)** A model of the coiled coil dimer based on PDB structure 2ZTA showing the F_{CN} and M_{Se} residues in stick format.[1] **(C)** A view of the structure displayed in **(B)** rotated 90°. **(D)** Helical-wheel diagram showing one heptad repeat. The heptad register designations ***a-g*** correspond to the heptad register in **(A)**.

Current methods for determining the K_D of coiled coils rely on the use of circular dichroism (CD); either by globally fitting thermal melting curves or by using the midpoint of the thermal unfolding transition (T_M) at several concentrations to determine the K_D.[10, 11] These methods are time consuming, relying on multiple melting experiments with precise control of concentration and peptide ratio required. They are also difficult to implement in a high throughput fashion and are not well suited for systems which do not undergo reversible thermal unfolding. Furthermore,

the sensitivity of CD limits the lowest concentration that can be studied. Fluorescence determination of K_D is the standard in protein-protein and protein-small molecule binding studies and could offer better ease of use and potentially higher accuracy than current methods for coiled coil systems. The potential for improvements in accuracy, ease of implementation and sensitivity make the application of fluorescence-based methods to coiled coil binding studies an attractive prospect, but current methods unfortunately suffer from drawbacks.

Tryptophan fluorescence is the obvious choice for an intrinsic fluorophore, owing to its relatively high quantum yield and sensitivity to the local environment. Trp fluorescence is widely used in studies of protein folding and protein-protein interactions as burial of a Trp sidechain leads to a shift in the emission maximum and often changes in quantum yield. However, the polyaromatic side chain of Trp is quite large relative to the coiled coil interface and may not be well-tolerated in these systems. Indeed, Trp is rarely found at interior positions in coiled coils.[12] Large, bright fluorophores such as Alexa dyes can be attached to the termini of coiled coils and assembly monitored by fluorescence resonance energy transfer (FRET), but are likely to perturb the system through aromatic-aromatic and hydrophobic interactions.

A smaller, unnatural fluorescent amino acid *p*-cyanophenylalanine (F_{CN}) offers a promising alternative. F_{CN} is structurally analogous to Tyr, with the hydroxyl group replaced by a nitrile functionality. The amino acid is smaller and hence less likely to perturb the coiled coil interface than tryptophan, and has a quantum yield and excitation and emission maxima that make it attractive for protein fluorescence applications. F_{CN} can be inserted into proteins either recombinantly, using an evolved aminoacyl-tRNA synthetase/tRNA pair or by solid phase peptide synthesis using standard Fmoc chemistry.[13-15] F_{CN} has two absorbance maxima at 233 and 280 nm, allowing it to be selectively excited in the presence of Trp or Tyr at 240 nm, which

corresponds to a minimum of Trp absorbance.[14, 15] F_{CN} fluorescence is modulated by solvation, increasing when the cyano group forms a hydrogen bond with the solvent and decreasing in aprotic, hydrophobic environments. F_{CN} is not expected to make a significant contribution to the CD signal at 222 nm and is likely to be less of a concern than Trp in this regard, as Trp has a more intense absorbance at 220 nm.[14]

Recent work has shown that F_{CN} fluorescence is strongly quenched by selenomethionine (M_{Se}), the selenium analogue of methionine, through an electron transfer mechanism.[16, 17] The sensitivity and short range of electron transfer mediated fluorescence quenching make it a valuable tool for protein structure studies, and Trp-His pairs have been extensively used in this manner.[18] However, His quenching is pH sensitive and requires the imidazole ring to be in the protonated state. In contrast, the quenching of F_{CN} by M_{Se} is independent of pH, extending the utility of the pair beyond the pH range accessible by protonated His.[16] Robust methods for the recombinant incorporation of M_{Se} have been developed because of its use in multi-wavelength anomalous dispersion (MAD) phasing in X-ray crystallography.[19] M_{Se} can also be incorporated into proteins using standard solid phase peptide synthesis methods. In this work we demonstrate the utility of the F_{CN}-M_{Se} pair to detect coiled coil formation in a sensitive, non-perturbing fashion and to measure the K_D of the interaction.

MATERIALS AND METHODS

Peptide Synthesis and Purification. Peptides were synthesized using standard 9-fluorenylmethyloxycarbonyl (Fmoc) chemistry on a CEM Liberty microwave peptide synthesizer. The C-terminus of each peptide was amidated through the use of 5-(4'-Fmoc-

aminomethyl-3',5-dimethoxyphenol)valeric acid (Fmoc-PAL-PEG-PS) resin. The N-termini of peptides were acetylated with acetic anhydride. Peptides were cleaved from resin in a cleavage cocktail of 5% thioanisole, 3.3% anisole and 3% 1,2-ethanedithiol in trifluoroacetic acid (TFA), filtered to remove resin and precipitated in cold ether. Peptides were pelleted by centrifugation at 10,000 rcf for 10 min, the supernatant was discarded, peptides were solubilized in 20% acetic acid (v/v) and lyophilized. Peptides were redissolved in 0.1% TFA (v/v) in 18 MΩ H_2O and purified by reverse-phase high performance liquid chromatography (HPLC) on a Higgins Analytical Proto 300 C18 10 μm preparative column (250x20 mm). A two buffer gradient system was used where buffer A was 0.1% TFA (v/v) in 18 MΩ H_2O and buffer B was 0.1% TFA in 9:1 acetonitrile:H_2O. Purity of the peptides was checked by HPLC on a Higgins Analytical Proto 300 C18 5 μm analytical column (250x4.6 mm). Peptides were characterized by matrix-assisted laser desorption/ionization time-of-flight (MALDI-TOF) mass spectrometry on a Bruker Daltonics autoflex TOF/TOF instrument. CC-19$F_{CN}A_N^{3.5}$ expected mass: 2907.588 Da (mono) observed: 2908.553 Da (mono). CC-19$WA_N^{3.5}$ expected mass: 2922.521 Da (mono) observed: 2923.394 Da (mono). CC-20$M_{Se}B_N^{3.5}$ expected mass: 2958.726 Da (mono) observed: 2959.409 Da (mono).

CD Measurements. CD wavelength scans were acquired on an Applied Photophysics Chirascan circular dichroism spectrometer. Measurements were performed in a 1 mm pathlength quartz cuvette from 190-260 nm in buffer or from 210-260 nm in urea using a 1 nm step size. Spectra were recorded as the average of three scans with an averaging time of 0.5 s. Thermal denaturation curves were collected at 222 nm using a 1 mm pathlength quartz cuvette for the 200 and 100 μM samples, and a 10 mm pathlength quartz cuvette for the 50, 20 and 10 μM samples.

The temperature was ramped from 2-94 °C in 2 °C steps with 120 s equilibration times and a 60 s averaging time. Thermal unfolding data was fit to equation (1).

$$\theta_{222} = \frac{a_n + b_n T + (a_d + b_d T) e^{\left(-\frac{\Delta G^\circ}{RT}\right)}}{1 + e^{\left(-\frac{\Delta G^\circ}{RT}\right)}} \quad (1)$$

Where θ_{222} is the ellipticity at 222 nm in millidegrees, a_n, b_n, a_d and b_d are fitting parameters defining the pre- and post-transition baseline, T is the temperature in K, R is the gas constant in kcal mol^{-1} K^{-1}, and ΔG° is the change in free energy upon unfolding in kcal mol^{-1}, determined from the Gibbs-Helmholtz equation (2).

$$\Delta G^\circ = \Delta H^\circ \left(1 - \frac{T}{T_M}\right) + \Delta C_p{}^\circ \left(T - T_M - T \ln\left(\frac{T}{T_M}\right)\right) \quad (2)$$

Where ΔG° is the change in free energy upon unfolding in kcal mol^{-1}, ΔH° is the change in enthalpy upon unfolding in kcal mol^{-1}, T is the temperature in K, T_M is the midpoint of the thermal unfolding transition in K and $\Delta C_p{}^\circ$ is the change in heat capacity upon unfolding in kcal mol^{-1} K^{-1}.

Fluorescence Measurements. Fluorescence emission spectra were acquired on a Photon Technologies International fluorimeter using a 10x10 mm quartz cuvette and a slit width of 1 mm (F_{CN} experiments) or 0.9 mm (Trp experiments). Spectra were recorded as the average of two scans (dimerization experiments) or four scans (K_D determination experiments) from 260-400 nm with an excitation wavelength of 240 nm (F_{CN} experiments) or from 300-450 nm with an excitation wavelength of 280 nm (Trp experiments), a step size of 1 nm and an averaging time of 0.5 s.

Determination of Dissociation Constant. *Circular Dichroism.* A dimer sample solution of CC-19F$_{CN}$A$_N^{3.5}$ and CC-20M$_{Se}$B$_N^{3.5}$ (100 μM each) in phosphate buffer (10 mM, pH 7.4) was prepared by mixing solutions of CC-19F$_{CN}$A$_N^{3.5}$ (200 μM, determined by absorbance at 280 nm) and CC-20M$_{Se}$B$_N^{3.5}$ (200 μM, determined by absorbance at 280 nm) in phosphate buffer. Additional dimer sample solutions at 100, 50, 20 and 10 μM total peptide concentration were prepared by serial dilution with phosphate buffer. The value of K_D was determined using the method of Marky and Breslauer as implemented for coiled coils by Woolfson and coworkers.[10, 11] T_M was measured as a function of total peptide concentration [*CC*] (note that [*CC*] denotes the total peptide concentration, not the concentration of the dimer) by fitting individual thermal melts to equation (1). Using the van 't Hoff equation leads to a linear relationship between $1/T_M$ and [*CC*], equation (3).

$$\frac{1}{T_M} = \frac{R}{\Delta H^\circ}\ln[CC] + \frac{\Delta S^\circ - R\ln 4}{\Delta H^\circ} \quad (3)$$

Where T_M is the midpoint of the thermal unfolding transition in K, ΔS° is the change in entropy upon unfolding in kcal mol^{-1} K^{-1}, R is the gas constant in kcal mol^{-1} K^{-1}, [*CC*] is the total concentration of coiled coil peptides in M and ΔH° is the change in enthalpy upon unfolding in kcal mol^{-1}. At T_M the fraction of molecules which are folded is 0.5, hence

$$\frac{1}{K_D^{T_M}} = \frac{4}{[CC]} \quad (4)$$

Where $K_D^{T_M}$ is the K_D at T_M. These relationships allow one to determine the total concentration of peptide, and thus the K_D, that would give a T_M equal to the temperature of interest.

Fluorescence. A sample solution of CC-19$F_{CN}A_N^{3.5}$ (412 nM) was prepared by diluting a stock solution of CC-19$F_{CN}A_N^{3.5}$ in H_2O (82 μM, determined by absorbance at 280 nm) with phosphate buffer (10 mM, pH 7.4). A dimer solution of CC-19$F_{CN}A_N^{3.5}$ and CC-20$M_{Se}B_N^{3.5}$ (403 nM and 64 μM, respectively) was prepared by diluting a stock solution of CC-20$M_{Se}B_N^{3.5}$ in H_2O (2987 μM, determined by absorbance at 280 nm) with the solution of CC-19$F_{CN}A_N^{3.5}$ (412 nM) in phosphate buffer. Additional dimer sample solutions were prepared at CC-20$M_{Se}B_N^{3.5}$ concentrations of 32000, 16000, 8000, 4000, 2000, 1000, 512, 256, 128, 64, 32, 16, 8, 4, 2 and 1 nM by serial dilution with the 412 nM CC-19$F_{CN}A_N^{3.5}$ solution. The slight increase from 403 to 412 nM in the CC-19$F_{CN}A_N^{3.5}$ concentration over the course of the dilution was corrected for in the fitting procedure. The value of K_D was determined by plotting the fluorescence intensity at 291 nm versus the concentration of CC-20$M_{Se}B_N^{3.5}$ and fitting to equation (5).

$$F_{291} = m[Tyr] + F_{max} + (F_{min} - F_{max})\left(\frac{([M_{Se}]+[F_{CN}]+K_D)-\sqrt{([M_{Se}]+[F_{CN}]+K_D)^2-4[F_{CN}][M_{Se}]}}{2[F_{CN}]}\right) \quad (5)$$

Where F_{291} is the fluorescence intensity at 291 nm, m is the concentration dependence of the fluorescence intensity of tyrosine at 291 nm, [Tyr] is the concentration of tyrosine in nM (equal to the concentration of CC-20$M_{Se}B_N^{3.5}$ in the present case), F_{max} is the maximal fluorescence intensity at 291 nm, F_{min} is the minimum fluorescence intensity at 291 nm, [M_{Se}] is the concentration of CC-20$M_{Se}B_N^{3.5}$ in nM, [F_{CN}] is the concentration of CC-19$F_{CN}A_N^{3.5}$ in nM, and K_D is the dissociation constant of the coiled coil dimer in nM.

RESULTS

Design of Coiled Coils. The coiled coil system used in this study was based on the parallel heterodimeric coiled coils designed by Thomas *et al.*[10] The pair was formed by two 27-residue peptides encompassing 3.5 heptad repeats with a hydrophobic interface composed of Leu and Ile

residues (Figure 1). Heterodimerization was enforced by charge complementarity: one of the peptides was acidic, rich in Asp and the other basic, rich in Lys. The expected net charges on the two peptides at pH 7.0 are -4 and +9, respectively. A single Asn residue at position 13 in each peptide locked the system into a parallel geometry stabilized by Asn-Asn H-bonding. The short range of M_{Se} quenching requires the Se atom to closely approach the aromatic ring of the F_{CN} residue. This could theoretically be accomplished by introducing the pair of residues at either the ***g*** and ***a*** or ***d*** and ***e*** positions in the heptad. A model based on PDB structure 2ZTA suggests that the ***ga*** arrangement offers slightly better geometry for the interaction, so F_{CN} was introduced at position 19 in the acidic peptide and M_{Se} was introduced at position 20 in the basic peptide.[1] Measurements on an idealized model of this system suggest a distance between the center of the Se atom and the center of the F_{CN} ring of 4.6 Å (Figure 1). The fractional solvent accessibility of the F_{CN} side chain in the dimer is 70% relative to an extended peptide, and the cyano group is fully exposed to solvent in the model structure. A single Tyr residue was incorporated at position 4 in the basic (M_{Se}) peptide to allow the concentration of the peptide to be determined by UV absorbance. The site was chosen to place the Tyr side chain as far as possible from the F_{CN} residue to limit FRET effects.[15] Measurements based on an idealized model of this system suggest a distance between the aromatic rings of the Tyr and F_{CN} residues of 26 Å. The N termini of the peptides were acetylated and the C termini amidated to increase stability of the dimer.

The Designed Coiled Coil Adopts Helical Structure. Coiled coil formation was characterized by circular dichroism (CD) spectroscopy. Individual peptides (35 μM) in phosphate buffer (10 mM, pH 7.4) show little α-helical structure as indicated by the molar ellipticity at 222 nm relative to the value at 200 nm (Figure 2). The fluorescent (acidic) and quenching (basic) peptides appear to adopt very similar disordered conformations as estimated by CD. In contrast, the CD spectrum

of a solution of both peptides (17.5 μM each) in the same buffer reveals significant helical structure, indicated by intense negative molar ellipticity at 222 and 208 nm as well as intense positive molar ellipticity at 193 nm. Denaturing the samples with urea (10 M) abolished the helical CD signal for both the monomeric peptides and the heterodimeric coiled coil (Figure S1). These results indicate that α-helix formation is strongly tied to heterodimeric association for these peptides, and that the introduction of F_{CN} and M_{Se} at the peptide interface does not prevent dimerization.

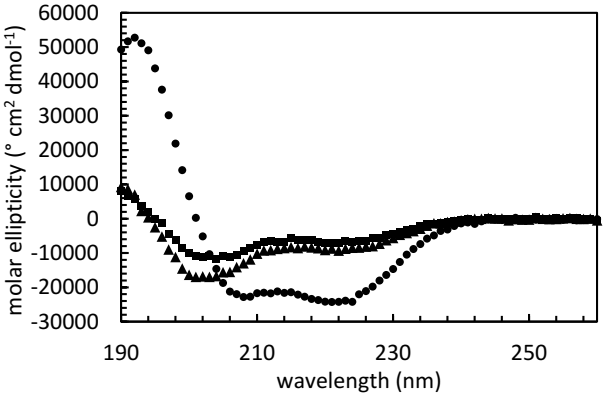

Figure 2. Circular dichroism spectra of CC-19$F_{CN}A_N^{3.5}$ (triangles), CC-20$M_{Se}B_N^{3.5}$ (squares) and the dimer (circles) in phosphate buffer (10 mM, pH 7.4) at 20 °C with a 35 μM total peptide concentration.

***p*-Cyanophenylalanine Fluorescence Quenching Provides a Sensitive Probe of Coiled Coil Formation.** The quenching efficiency of M_{Se} in the coiled coil system was examined by comparing the emission spectrum of the F_{CN} monomer (35 μM) in phosphate buffer (10 mM, pH 7.4) to the spectrum of a sample that contained both peptides (35 μM each) in the same buffer (Figure 3). We avoided the use of chloride salts since chloride can quench F_{CN} fluorescence.[20] F_{CN} was excited at 240 nm to minimize any contribution from the Tyr residue in CC-20$M_{Se}B_N^{3.5}$. Fluorescence intensity at the emission maximum (291 nm) was 81% lower in the dimer sample compared to the

F_{CN} peptide alone, indicating a high quenching efficiency. The quenching effect was abolished by denaturing the coiled coil with urea (10 M), returning the intensity to the same value observed for the isolated F_{CN} peptide in either buffer or 10 M urea (Figure S2).

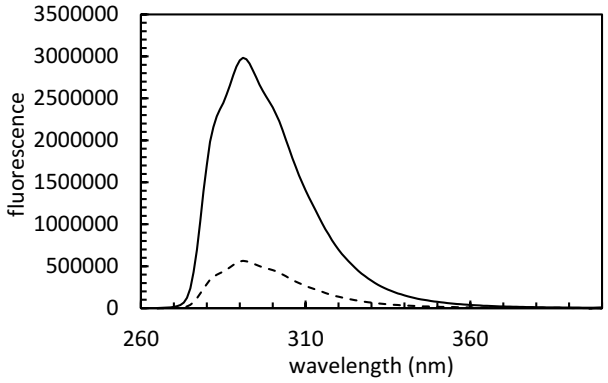

Figure 3. Fluorescence emission spectra of CC-19$F_{CN}A_N^{3.5}$ (solid line) and the dimer with CC-20$M_{Se}B_N^{3.5}$ (dashed line) in phosphate buffer (10 mM, pH 7.4) at 20 °C with a CC-19$F_{CN}A_N^{3.5}$ concentration of 35 μM. The excitation wavelength was 240 nm.

Tryptophan Fluorescence is Much Less Sensitive to Coiled Coil Formation. Although the use of F_{CN} appears quite promising, we also investigated the use of Trp as the fluorophore in the coiled coil system. The peptides used for this pair were identical to those that made up the F_{CN}-M_{Se} pair with the only change being the replacement of F_{CN} with Trp; this peptide was designated CC-19W$A_N^{3.5}$ (Figure 4). Measurements on a model based on PDB structure 2ZTA suggest a distance between the center of the Se atom and the center of the indole ring of 5.0 Å.[1] The Trp-M_{Se} heterodimer was characterized by CD spectroscopy (Figure S3). As with the F_{CN}-M_{Se} pair, the monomeric peptides appeared to be largely unstructured, with only weak helical structure as indicated by CD. In contrast, strong negative ellipticity was observed at 222 and 208 nm as well as intense positive ellipticity at 193 nm in a mixed peptide solution, as was observed for the F_{CN}-M_{Se} pair, consistent with coiled coil formation. Denaturing the samples with urea (10 M) abolished

the helical CD signal for both the monomeric peptides and the heterodimeric coiled coil (Figure S4).

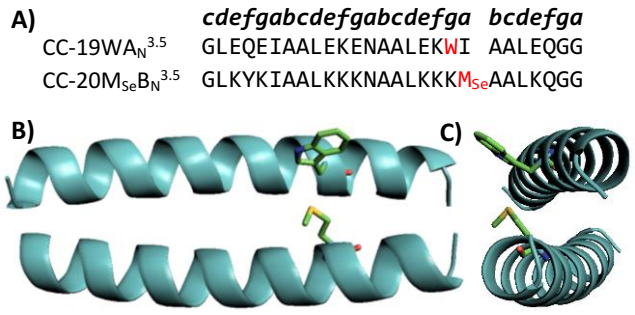

Figure 4. (A) Sequences and heptad register of the CC-19WA$_N^{3.5}$ and CC-20M$_{Se}$B$_N^{3.5}$ coiled coil peptides. M$_{Se}$ denotes selenomethionine. **(B)** A model of the coiled coil dimer based on PDB structure 2ZTA showing the Trp and M$_{Se}$ residues in stick format.[1] **(C)** A view of the structure displayed in **(B)** rotated 90°.

The fluorescence quenching efficiency of the Trp-M$_{Se}$ pair was also examined, but only a weak 14% quenching effect was observed in the mixed peptide solution (35 μM each) compared to a 35 μM solution of CC-19WA$_N^{3.5}$ (Figure 5). The weaker quenching could result from less optimal geometry in the Trp-M$_{Se}$ coiled coil, lower intrinsic quenching efficiency of M$_{Se}$ for Trp relative to F$_{CN}$, the quenching effect being partially offset by the intrinsic increase in Trp fluorescence due to partial burial, proximity of the indole ring to a Lys sidechain in both the folded and unfolded states, as Lys can quench Trp fluorescence, or some combination of these effects.

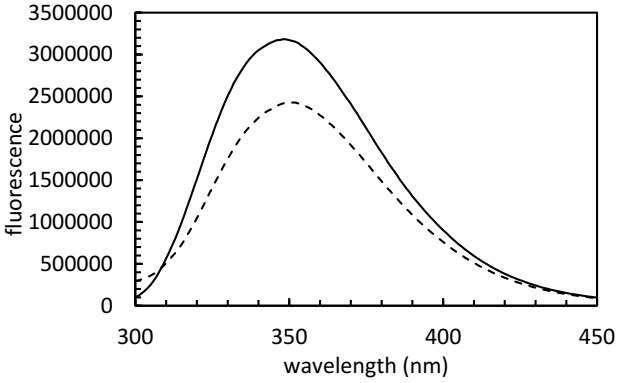

Figure 5. Fluorescence emission spectra of CC-19WA$_N^{3.5}$ (solid line) and the dimer with CC-20M$_{Se}$B$_N^{3.5}$ (dashed line) in phosphate buffer (10 mM, pH 7.4) at 20 °C with a CC-19WA$_N^{3.5}$ concentration of 35 μM. The excitation wavelength was 280 nm.

Fluorescence Monitored Titrations Provide a Convenient and Accurate Method to Determine K_D. The dissociation constant for the heterodimer was first determined using a standard CD method for coiled coils. Solutions of the heterodimer were prepared in phosphate buffer (10 mM, pH 7.4) at 202, 101, 49, 19 and 8 μM (1:1 peptide concentration ratio, concentration determined by absorbance at 280 nm). CD-monitored thermal denaturation experiments were performed for each of these samples and the unfolding transition midpoint (T_M) was determined using standard methods (Figure S5). The K_D was calculated using the method of Marky and Breslauer.[11] $1/T_M$ was plotted versus the natural logarithm of the total concentration of coiled coil peptides and fit to equation (3).

Analysis of the thermally induced unfolding of coiled coils has often assumed that the $\Delta C_p°$ is zero or small.[10] The linear van 't Hoff plot is consistent with this, however the value of $\Delta C_p°$ can also enter into the analysis of the fits of the individual melting curves. For samples that have a high T_M, ie. samples with high total peptide concentration [*CC*], the post-transition baseline may not

always be well defined. In this case, the apparent T_M derived from the non-linear fit to the melting curve can vary if $\Delta C_p°$ is fixed at different values. This likely reflects the fact that curves with a poorly defined post-transition baseline are being fit with seven variables; two for each baseline, T_M, $\Delta H°$, and $\Delta C_p°$. This potential complication is less of an issue when the pre- and post-transition baselines are well defined (Figure S6).

We analyzed the individual thermal unfolding curves using a range of fixed values of $\Delta C_p°$ to generate apparent values of T_M as a function of [*CC*]. Using these values in equation (3) leads to a modest variation in K_D. Using $\Delta C_p° = 0$ kcal mol^{-1} K^{-1} to fit the thermal melts leads to a K_D of 24.7 nM while a value of 0.20 kcal mol^{-1} K^{-1} leads to a K_D of 10.3 nM. An alternative approach is to perform a global analysis of all five melting curves, allowing $\Delta C_p°$ to be determined as a fitting variable that is constant across all experiments. The value of $\Delta C_p°$ determined in this analysis was 0.58 kcal mol^{-1} K^{-1}, which leads to a K_D value of 1.67 nM (Figure 6). This value of $\Delta C_p°$ is in excellent agreement with the theoretical value of 0.55 kcal mol^{-1} K^{-1} predicted by the empirical relationship between $\Delta C_p°$ and the number of residues in a protein.[21] The value of K_D determined using the theoretical $\Delta C_p°$ value of 0.55 kcal mol^{-1} K^{-1} is 2.27 nM. Given that the changes in the peptide sequences likely result in a slight perturbation of the dimer interface, these values are in good agreement with the K_D of 5.15 nM determined for the parent peptides by Thomas *et al.*[10]

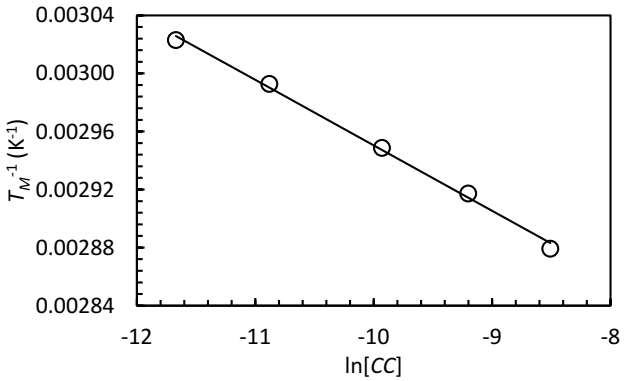

Figure 6. The inverse of the thermal unfolding transition midpoints (T_M) determined using a $\Delta C_p°$ value of 0.58 kcal mol^{-1} K^{-1} for 1:1 mixtures of CC-19F$_{CN}$A$_N^{3.5}$ and CC-20M$_{Se}$B$_N^{3.5}$ at total peptide concentrations of 202, 101, 49, 19 and 8 μM plotted against the natural logarithm of the peptide concentration in M (circles). The solid line is a linear fit of the data to equation (3), $R^2 = 0.9970$, p = 0.0000688.

Having measured K_D by CD based methods we then tested if the F$_{CN}$-M$_{Se}$ pair can be exploited to give an accurate determination of K_D. Fluorescence emission of F$_{CN}$ was monitored at a fixed concentration of CC-19F$_{CN}$A$_N^{3.5}$ as the concentration of CC-20M$_{Se}$B$_N^{3.5}$ was varied (Figure 7). The fluorescence intensity at 291 nm (F_{291}) was plotted against the concentration of CC-20M$_{Se}$B$_N^{3.5}$, [M_{Se}], and a typical binding isotherm was observed for CC-20M$_{Se}$B$_N^{3.5}$ below 3 μM. At high CC-20M$_{Se}$B$_N^{3.5}$ concentrations the F$_{CN}$ fluorescence is effectively quenched and the weaker Tyr fluorescence contributes significantly to the observed intensity at 291 nm, possibly from limited excitation of Tyr at 240 nm. This leads to an increase in the observed fluorescence at high concentrations of the M$_{Se}$ peptide. This effect is trivial to model and correct for with a linear function dependent on the concentration of the M$_{Se}$ peptide. The plot of F_{291} versus [M_{Se}] was fit to equation (5) with m, F_{max}, F_{min} and K_D as fitting parameters. The value of K_D determined using this procedure was 16.7 nM, which is in excellent agreement with the values determined by CD assuming $\Delta C_p°$ values of 0.0 to 0.2 kcal mol^{-1} K^{-1} and is reasonable agreement to the value determined by the global analysis of the CD-monitored thermal melts. We also fit the fluorescence data using a truncated data set which excluded data collected for CC-20M$_{Se}$B$_N^{3.5}$ concentrations above 2 μM. This choice restricts the data to a range where the post-transition baseline is constant. The data were fit to a modified version of equation (5) which did not include the Tyr correction

term. This analysis yielded a K_D of 14.8 nM, which is in excellent agreement with the value determined using the more robust method.

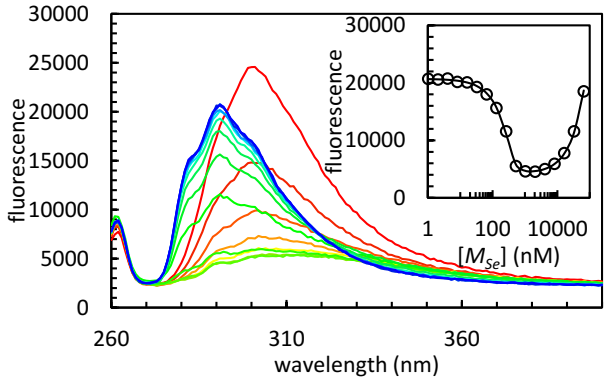

Figure 7. Fluorescence emission spectra of CC-19$F_{CN}A_N^{3.5}$ (412 nM) in phosphate buffer (10 mM, pH 7.4) at 20 °C in the presence of increasing concentrations of the CC-20$M_{Se}B_N^{3.5}$ (blue to red). The excitation wavelength was 240 nm. **Inset:** The fluorescence intensity at 291 nm is plotted against the concentration of CC-20$M_{Se}B_N^{3.5}$ (open circles) and fit to equation (5).

DISCUSSION

The data presented here demonstrates the utility of F_{CN}-M_{Se} pairs to quantitatively monitor coiled coil formation. The pair has the advantage of being sensitive and non-perturbing. A third advantage is that the detection limit is clearly lower than is possible with CD. This will be of particular use when one needs to determine K_D values for strongly binding systems. The fluorescence based approach also avoids any difficulties due to irreversible thermal unfolding. The fluorescence quenching method also avoids the problems associated with the large number of fitting variables inherent in the CD method used here. In particular, varying the value of $\Delta C_p°$ (which can be determined, but requires additional experiments) from 0 to 0.58 kcal mol^{-1} K^{-1} changes the value of K_D from 24.7 to 1.67 nM. Although this level of uncertainty may not be an issue in all applications, the fluorescence quenching method avoids it altogether. This aspect of the CD fitting

problem can be circumvented by taking the second derivative of very high quality thermal unfolding data to determine T_M. We were unable to use this method to analyze our data because of signal-to-noise issues, but the fluorescence method again avoids this problem.

The M_{Se}-F_{CN} approach also suffers from some potential disadvantages relative to the CD based approaches. M_{Se} is expected to be more prone to oxidation than Met, although no oxidation was detected in the system studied here, and the fluorescence quenching properties of oxidized M_{Se} derivatives have not been investigated. An oxidized M_{Se} residue is larger than M_{Se} and thus might affect packing. Reducing agents and degassed buffers can be used if oxidation is a potential concern. There are some additional practical considerations if F_{CN} fluorescence quenching is employed. F_{CN} fluorescence is quenched by Cl^- ions, thus high concentrations of Cl^- containing buffers should be avoided.

Fluorescence-based methods are well suited to high throughput assays, while CD generally is not. The F_{CN}-M_{Se} pair offers a fluorescence probe that is amenable to screening libraries of coiled coils. For example, a single F_{CN} containing peptide could be screened against a library of M_{Se} containing peptides. Another useful feature is that, unlike for Trp-His pairs, the quenching effect is independent of pH.[16] In principle the F_{CN}-M_{Se} pair can be used to follow thermally induced dissociation, however F_{CN} fluorescence has a significant intrinsic temperature dependence which may complicate or compromise the analysis. The data analyzed in this work was collected using peptides prepared by solid phase peptide synthesis, but both F_{CN} and M_{Se} can be incorporated into proteins using well established recombinant methods, thus the methodology is not limited to synthetic peptides. The use of F_{CN}-M_{Se} pairs is not limited to coiled coils and can be used to quantitatively monitor other protein-protein interactions and self-assembly processes.

ASSOCIATED CONTENT

Supporting Information Available.

Additional figures, CD spectra, CD thermal denaturation curves, fluorescence emission spectra.

This material is available free of charge via the Internet at http://pubs.acs.org.

AUTHOR INFORMATION

Corresponding Author

*daniel.raleigh@stonybrook.edu; Tel 631 632 9547

Author Contributions

The manuscript was written through contributions of all authors. All authors have given approval to the final version of the manuscript.

Funding Sources

This work was supported by NSF MCB-1330259 grant to DPR.

ACKNOWLEDGMENT

The authors thank Prof. Feng Gai for his encouragement and helpful discussions and Mr. Zachary Ridgway for critically reading the manuscript.

ABBREVIATIONS

K_D, dissociation constant; CD, circular dichroism; F_{CN}, *p*-cyanophenylalanine; M_{Se}, selenomethionine; T_M, midpoint of thermal unfolding transition; FRET, Förster resonance energy transfer.

REFERENCES

[1] Oshea, E. K., Klemm, J. D., Kim, P. S., and Alber, T. (1991) X-ray structure of the GCN4 leucine zipper, a 2-stranded, parallel coiled coil, *Science 254*, 539-544.

[2] Rackham, O. J., Madera, M., Armstrong, C. T., Vincent, T. L., Woolfson, D. N., and Gough, J. (2010) The evolution and structure prediction of coiled coils across all genomes, *J Mol Biol 403*, 480-493.

[3] Oneil, K. T., and Degrado, W. F. (1990) A thermodynamic scale for the helix-forming tendencies of the commonly occurring amino-acids, *Science 250*, 646-651.

[4] Negron, C., and Keating, A. E. (2014) A set of computationally designed orthogonal antiparallel homodimers that expands the synthetic coiled-coil toolkit, *J Am Chem Soc 136*, 16544-16556.

[5] Root, M. J., Kay, M. S., and Kim, P. S. (2001) Protein design of an HIV-1 entry inhibitor, *Science 291*, 884-888.

[6] Boyle, A. L., and Woolfson, D. N. (2011) De novo designed peptides for biological applications, *Chem Soc Rev 40*, 4295-4306.

[7] Woolfson, D. N. (2005) The design of coiled-coil structures and assemblies, *Adv Protein Chem 70*, 79-+.

[8] Morais, A. C., and Ferreira, S. T. (2005) Folding and stability of a coiled-coil investigated using chemical and physical denaturing agents: comparative analysis of polymerized and non-polymerized forms of alpha-tropomyosin, *Int J Biochem Cell Biol 37*, 1386-1395.

[9] Wagner, D. E., Phillips, C. L., Ali, W. M., Nybakken, G. E., Crawford, E. D., Schwab, A. D., Smith, W. F., and Fairman, R. (2005) Toward the development of peptide nanofilaments and nanoropes as smart materials, *Proc Natl Acad Sci U S A 102*, 12656-12661.

[10] Thomas, F., Boyle, A. L., Burton, A. J., and Woolfson, D. N. (2013) A set of de novo designed parallel heterodimeric coiled coils with quantified dissociation constants in the micromolar to sub-nanomolar regime, *J Am Chem Soc 135*, 5161-5166.

[11] Marky, L. A., and Breslauer, K. J. (1987) Calculating thermodynamic data for transitions of any molecularity from equilibrium melting curves, *Biopolymers 26*, 1601-1620.

[12] Woolfson, D. N., and Alber, T. (1995) Predicting oligomerization states of coiled coils, *Protein Sci 4*, 1596-1607.

[13] Miyake-Stoner, S. J., Miller, A. M., Hammill, J. T., Peeler, J. C., Hess, K. R., Mehl, R. A., and Brewer, S. H. (2009) Probing protein folding using site-specifically encoded unnatural amino acids as FRET donors with tryptophan, *Biochemistry 48*, 5953-5962.

[14] Tucker, M. J., Oyola, R., and Gai, F. (2005) Conformational distribution of a 14-residue peptide in solution: a fluorescence resonance energy transfer study, *J Phys Chem B 109*, 4788-4795.

[15] Taskent-Sezgin, H., Chung, J., Patsalo, V., Miyake-Stoner, S. J., Miller, A. M., Brewer, S. H., Mehl, R. A., Green, D. F., Raleigh, D. P., and Carrico, I. (2009) Interpretation of p-cyanophenylalanine fluorescence in proteins in terms of solvent exposure and contribution of side-chain quenchers: a combined fluorescence, IR and molecular dynamics study, *Biochemistry 48*, 9040-9046.

[16] Peran, I., Watson, M. D., Bilsel, O., and Raleigh, D. P. (2016) Selenomethionine, p-cyanophenylalanine pairs provide a convenient, sensitive, non-perturbing fluorescent probe of local helical structure, *Chem Commun 52*, 2055-2058.

[17] Mintzer, M. R., Troxler, T., and Gai, F. (2015) p-Cyanophenylalanine and selenomethionine constitute a useful fluorophore-quencher pair for short distance measurements: application to polyproline peptides, *Phys Chem Chem Phys 17*, 7881-7887.
[18] Lakowicz, J. R. (2006) *Principles of fluorescence spectroscopy*, 3rd ed., Springer, New York.
[19] Hendrickson, W. A. (1991) Determination of macromolecular structures from anomalous diffraction of synchrotron radiation, *Science 254*, 51-58.
[20] Pazos, I. M., Roesch, R. M., and Gai, F. (2013) Quenching of p-cyanophenylalanine fluorescence by various anions, *Chem Phys Lett 563*, 93-96.
[21] Myers, J. K., Pace, C. N., and Scholtz, J. M. (1995) Denaturant m values and heat capacity changes: relation to changes in accessible surface areas of protein unfolding, *Protein Sci 4*, 2138-2148.

Table of Contents Graphic

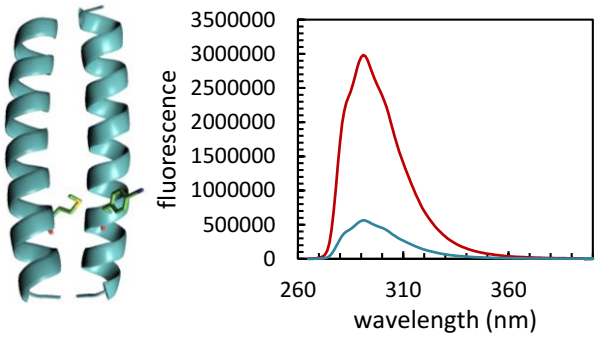

Supporting Information For

A Non-perturbing Probe of Coiled Coil Formation Based on Electron Transfer Mediated Fluorescence Quenching

Matthew D. Watson, Ivan Peran, Daniel P. Raleigh

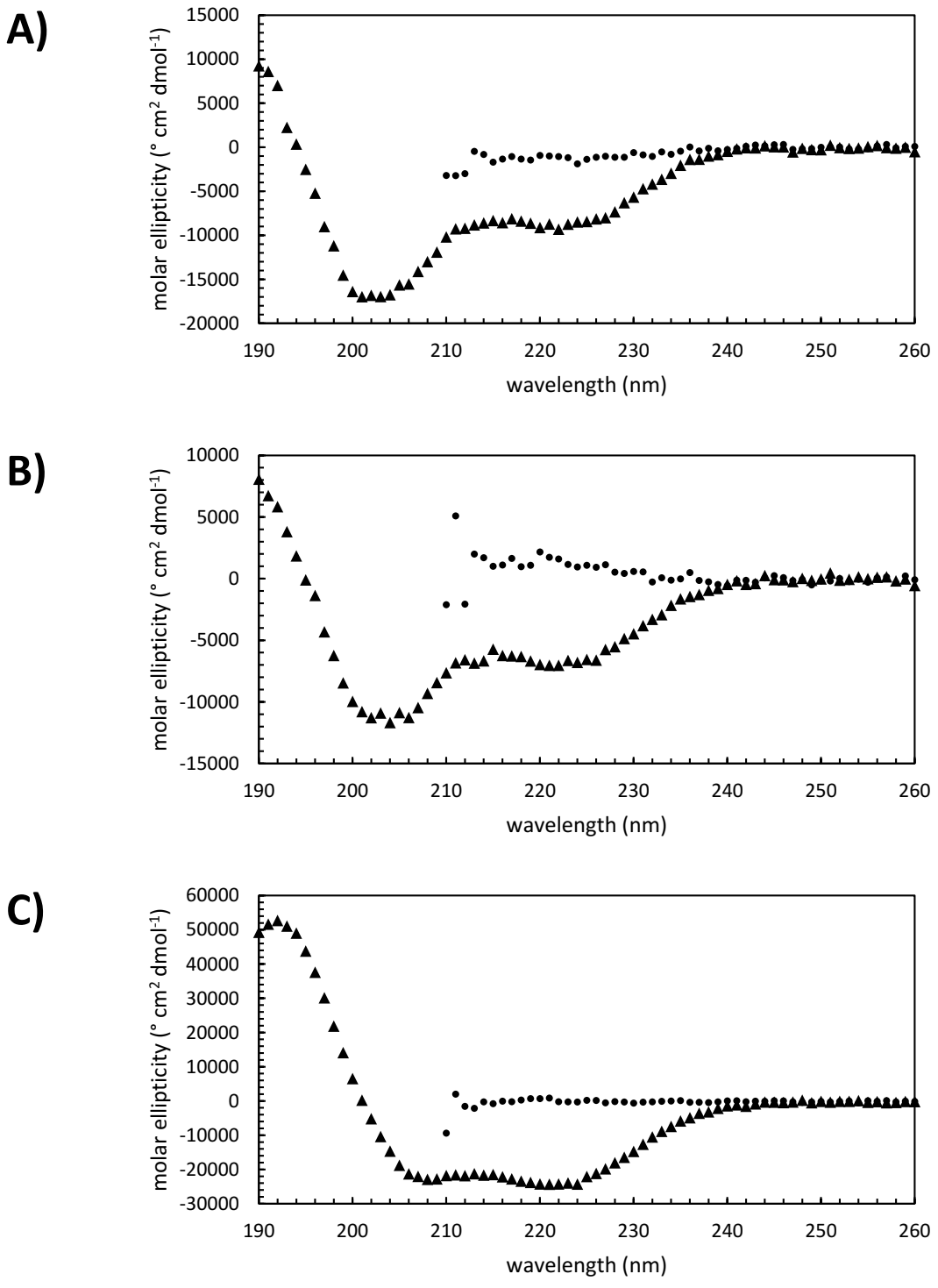

Figure S1. (A) Circular dichroism spectra of CC-19$F_{CN}A_N^{3.5}$ (35 µM) at 20 °C in phosphate buffer (10 mM, pH 7.4, triangles) and in urea (10 M, circles). **(B)** Circular dichroism spectra of CC-20$M_{Se}B_N^{3.5}$ (35 µM) at 20 °C in phosphate buffer (10 mM, pH 7.4, triangles) and in urea (10 M, circles). **(C)** Circular dichroism spectra of a mixed solution of CC-19$F_{CN}A_N^{3.5}$ and CC-20$M_{Se}B_N^{3.5}$ (1:1, 35 µM total peptide concentration) at 20 °C in phosphate buffer (10 mM, pH 7.4, triangles) and in urea (10 M, circles).

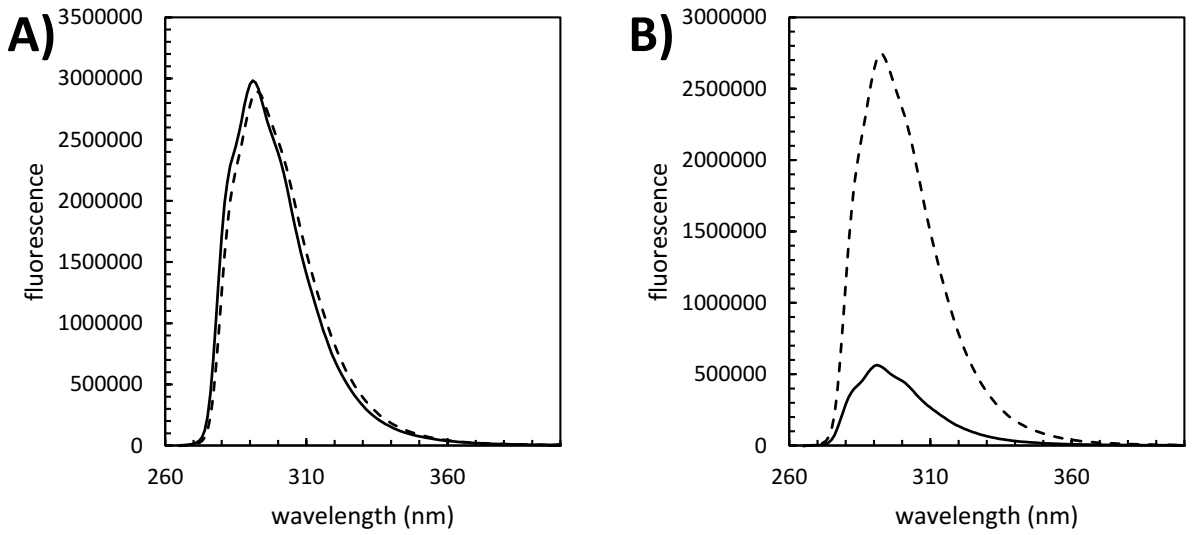

Figure S2. (A) Fluorescence emission spectra of CC-19$F_{CN}A_N^{3.5}$ (35 µM) at 20 °C in phosphate buffer (10 mM, pH 7.4, solid line) and in urea (10 M, dashed line). The excitation wavelength used was 240 nm. **(B)** Fluorescence emission spectra of a mixed solution of CC-19$F_{CN}A_N^{3.5}$ and CC-20$M_{Se}B_N^{3.5}$ (1:1, 70 µM total peptide concentration) at 20 °C in phosphate buffer (10 mM, pH 7.4, solid line) and in urea (10 M, dashed line). The excitation wavelength used was 240 nm.

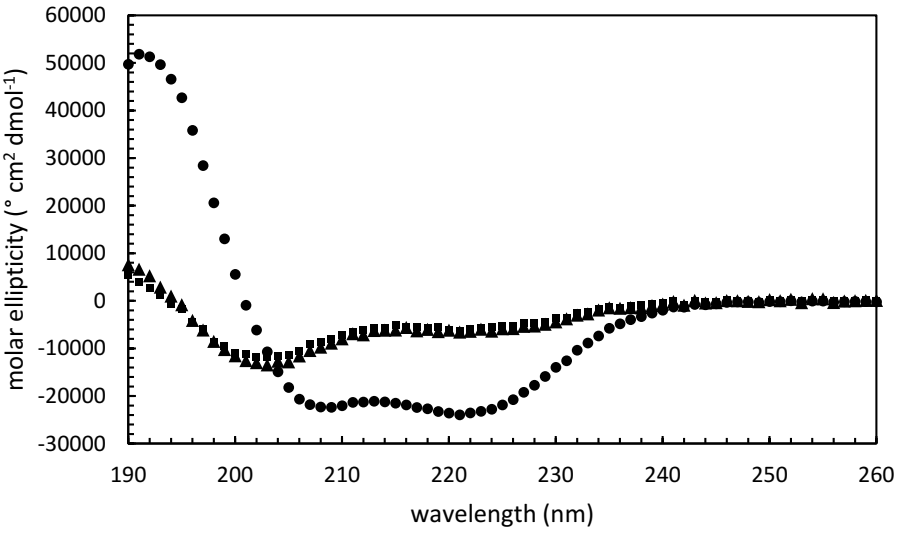

Figure S3. Circular dichroism spectra of CC-19W$A_N^{3.5}$ (triangles), CC-20$M_{Se}B_N^{3.5}$ (squares) and the dimer (circles) in phosphate buffer (10 mM, pH 7.4) at 20 °C with a 35 μM total peptide concentration.

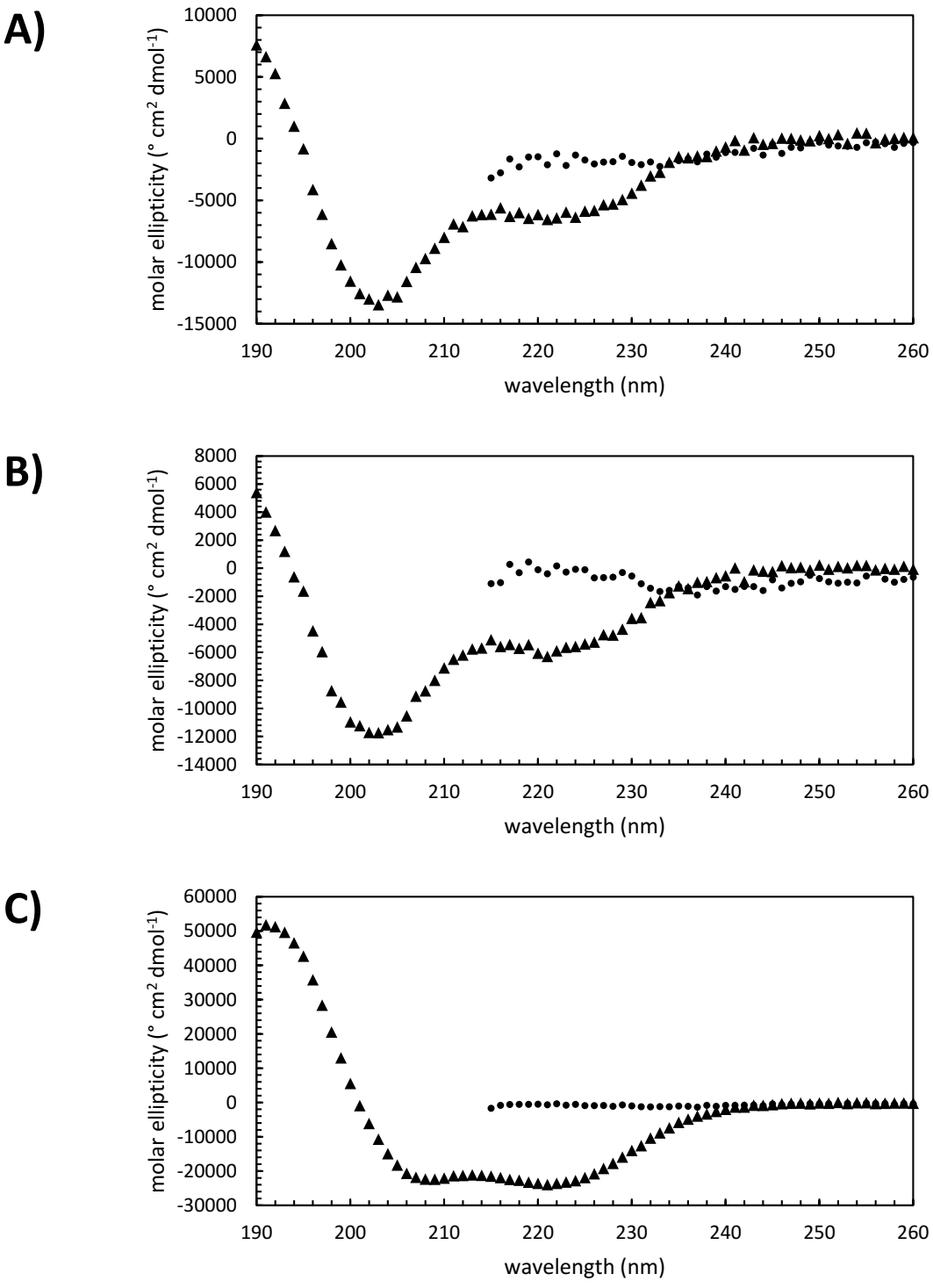

Figure S4. (A) Circular dichroism spectra of CC-19WA$_N^{3.5}$ (35 µM) at 20 °C in phosphate buffer (10 mM, pH 7.4, triangles) and in urea (10 M, circles). **(B)** Circular dichroism spectra of CC-20M$_{Se}$B$_N^{3.5}$ (35 µM) at 20 °C in phosphate buffer (10 mM, pH 7.4, triangles) and in urea (10 M, circles). **(C)** Circular dichroism spectra of a mixed solution of CC-19WA$_N^{3.5}$ and CC-20M$_{Se}$B$_N^{3.5}$ (1:1, 35 µM total peptide concentration) at 20 °C in phosphate buffer (10 mM, pH 7.4, triangles) and in urea (10 M, circles).

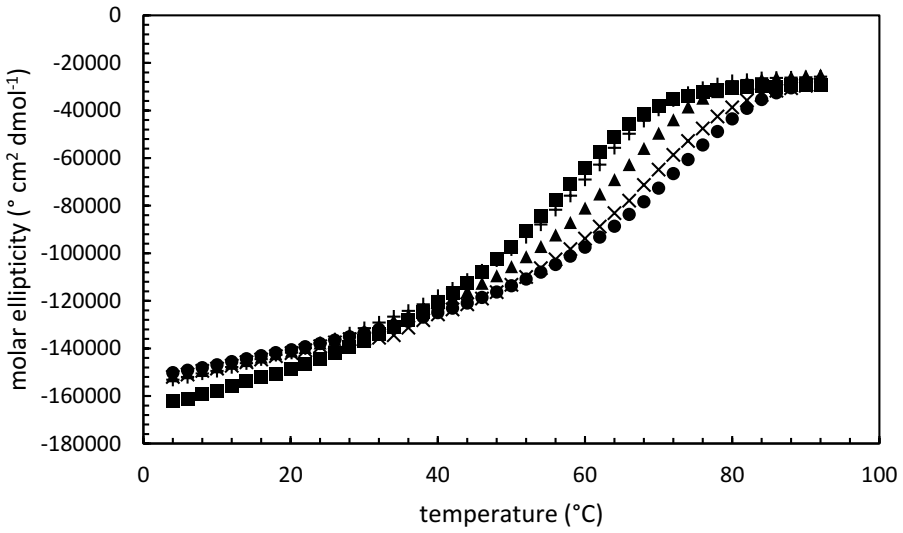

Figure S5. Circular dichroism monitored thermal unfolding curves for the CC-19$F_{CN}A_N^{3.5}$/CC-20$M_{Se}B_n^{3.5}$ dimer at 202 µM (circles), 101 µM (x), 49 µM (triangles), 19 µM (+) and 8 µM (squares). Experiments were performed in phosphate buffer (10 mM, pH 7.4) at 20 °C with a monomer ratio of 1:1. Curves were fit to equation (1) to determine T_M, the midpoint of the unfolding transition.

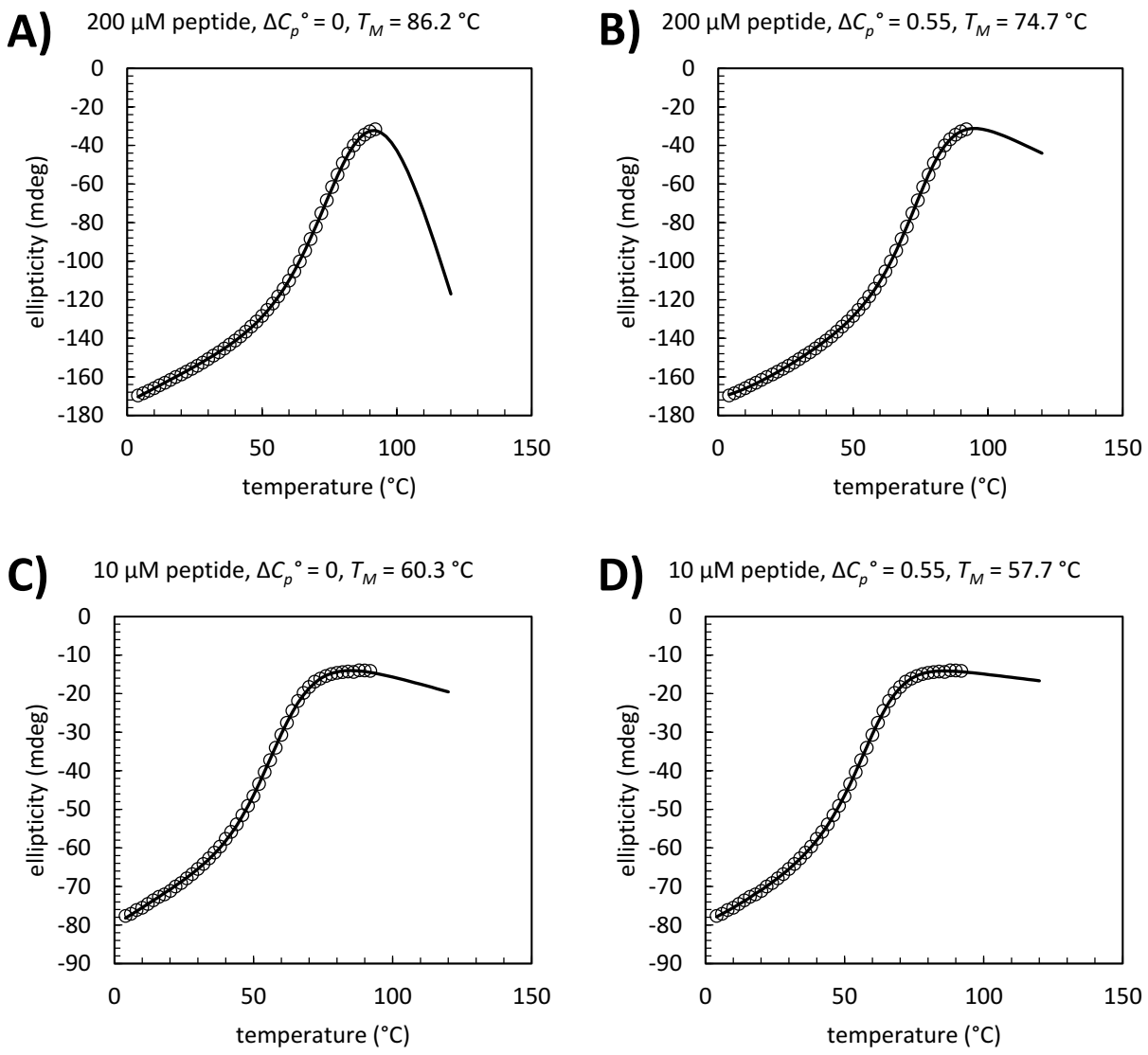

Figure S6. Dependence of apparent T_M values on the choice of ΔC_p° illustrated for [*CC*] = 200 µM and [*CC*] = 10 µM. **(A)** Fit to the 200 µM data with ΔC_p° = 0 kcal mol^{-1} K^{-1} yields a T_M of 86.2 °C, but also leads to a nonphysical post-transition baseline. **(B)** Fit to the 200 µM data with ΔC_p° = 0.55 kcal mol^{-1} K^{-1} yields T_M = 74.7 °C with a more reasonable post-transition baseline. **(C)** and **(D)** display fits to melting data collected at [*CC*] = 10 µM. The choice of ΔC_p° has less dramatic effects.